Far-Field Generation of Localized Light Fields using Absorbance Modulation

Rajesh Menon*
Research Laboratory of Electronics, Massachusetts Institute of Technology, Cambridge, Massachusetts 02139, USA

Hsin-Yu Tsai
Department of Electrical Engineering and Computer Science, Massachusetts Institute of Technology, Cambridge, Massachusetts 02139, USA

Samuel W. Thomas III
Department of Chemistry, Massachusetts Institute of Technology, Cambridge, Massachusetts 02139, USA
(Received 20 September 2006; published 25 January 2007)

In this Letter, we report the confinement of a uniform beam of light ($\lambda_1 = 400$ nm) at the nodes of a standing wave ($\lambda_2 = 532$ nm) via absorbance modulation. In the present implementation of absorbance modulation, a thin polymer film containing a photochromic azobenzene side chain is exposed to a standing wave at λ_2 and a uniform beam at λ_1, resulting in alternate regions of high and low absorbance. Light at λ_1 is localized around the low-absorbance regions. Using photoresist exposures, we mapped out the localized light intensity distribution, which agrees well with our theoretical model. Since the width of this distribution is primarily determined by the ratio of the intensities at the two wavelengths, this technique opens up the possibility of localizing light fields below the diffraction limit using far-field optics.

DOI: 10.1103/PhysRevLett.98.043905 PACS numbers: 42.25.Bs, 42.70.Gi, 42.70.Jk

Introduction.—Optical patterns are typically generated by projecting an image of a physical mask, by scanning one or more tightly focused spots [1], by scanning near-field probes [2,3], or by exposure through a contact mask [4]. The first two are far-field techniques, and hence, limited by diffraction. The resolution of such techniques can be increased by reducing the wavelength of illumination or by increasing the index of refraction [5,6], both of which often involve exceptional engineering challenges. In the last two techniques, sub–diffraction-limited patterning is possible, since the image is formed not only by the propagating low spatial frequencies but also by the evanescent high spatial frequencies. However, near-field scanning techniques are typically plagued by the requirement for tight control of the distance between the source of the evanescent fields and the recording medium, i.e., the gap. The use of materials with negative refractive index [7] or negative permittivity [8,9] can alleviate this problem, but not eliminate it. Even with the use of such materials, the gap typically remains less than 100 nm, which is often difficult to maintain accurately while scanning useful areas. Patterning with a contact mask can achieve high resolution [10,11], but suffers from the requirement that an accurate mask is required in intimate contact with the substrate. Any defects in the mask or the substrate surface has significant deleterious effects on the generated patterns.

The use of reversible saturable transitions was proposed to overcome these limitations [12]. Recently, this approach has had significant success in fluorescence microscopy [13]. We expanded on this idea, and proposed an alternative approach to the high-resolution recording of an optical pattern that uses an absorbance-modulation layer (AML) on top of the recording medium [14]. The AML is composed of photochromic molecules that reversibly change their absorbance upon exposure to light, i.e., illumination switches the molecule from an opaque configuration to a transparent one and vice versa. When exposed to a null at a long wavelength (λ_2), coincident with a beam of short wavelength (λ_1), a subwavelength transparent aperture is generated in the AML, as illustrated in the inset in Fig. 1. The size of the aperture is controlled primarily by the ratio of the intensities at the two wavelengths, and hence, not limited by the ''diffraction limit'' imposed by either one. In this Letter, we demonstrate the one-dimensional equivalent of the proposed technique. In particular, we exposed the AML to fringes formed by two-beam interference at $\lambda_2 = 532$ nm, and a uniform beam at $\lambda_1 = 400$ nm. Only the

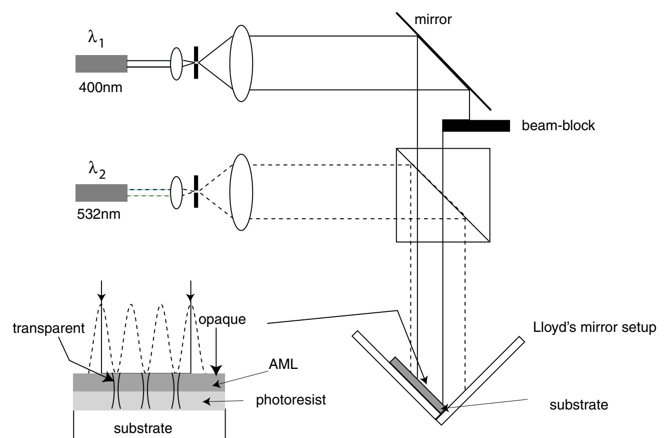

FIG. 1 (color online). Schematic of experimental setup. The standing-wave illumination at λ_2 creates a local aperture for λ_1, through which the underlying photoresist is exposed.

 © 2007 The American Physical Society

transmitted light at $\lambda_1 = 400$ nm exposes an underlying photoresist layer. We experimentally characterized the spatial structure of this localized light field, and compared it against the theoretical model. We further show that by choosing the appropriate ratio of power densities at the two wavelengths, the width of the transmitted lines can be significantly smaller than the diffraction limit. This technique, therefore, opens up the possibility of generating optical near fields with far-field optics.

Experiment.—The optical setup consisted of a Lloyd's mirror configuration, as depicted in Fig. 1. The output of a 532 nm laser was expanded and collimated, before impinging on the Lloyd's mirror and the substrate, resulting in a standing-wave pattern on the surface of the substrate. Light from a 400 nm laser was made coincident with the first beam by a polarizing beam splitter. A beam block was used to ensure that no 400 nm light was incident on the Lloyd's mirror. As a result, the substrate was illuminated by a standing wave at $\lambda_2 = 532$ nm, and a uniform beam at $\lambda_1 = 400$ nm. The beam profiles near the substrate were measured and the intensities near the optical axis at 400 nm and 532 nm were estimated as $1.7\ \text{mW/cm}^2$ and $6.4\ \text{mW/cm}^2$, respectively.

The substrate consisted of pieces of silicon wafer that were spin coated with 200 nm of antireflection coating, BarLi (Microchemicals, Germany), 150 nm of photoresist, PS-4 (Tokyo OHKA Kogyo Co., Ltd., Japan), 23 nm of poly vinyl alcohol (PVA), and 200 nm of azobenzene polymer in that order. After exposure, the azobenzene layer was removed by dipping in trichloroethylene for 30 s. This was followed by a 30 s rinse in DI water to remove the PVA layer. The PVA acts as a barrier layer, protecting the underlying photoresist during the removal of the azobenzene. It also prevents the intermixing of the azobenzene and the photoresist. The substrate was then baked on a hotplate at 115 °C for 90 s to initiate the cross linking of the exposed photoresist. PS-4 is a negative photoresist, so only the unexposed regions are removed upon development. Finally, the substrate was developed in CD-26 (0.26N tetramethylammonium hydroxide, Shipley, U.S.A.) for 60 s. The developed patterns in photoresist were sputter coated with about 1 nm of a Ti/Au alloy before inspection in a scanning-electron microscope.

The composition of the azobenzene polymer is shown in Fig. 2. The synthesis of the monomers and the polymerization process have been described elsewhere [15,16]. Upon exposure to $\lambda_1 = 400$ nm, the trans isomer undergoes a photoisomerization reaction forming the cis isomer. The reverse reaction is favored upon exposure to $\lambda_1 = 532$ nm. The cis isomer is also thermally unstable, slowly converting back to trans. The absorbance (at $\lambda_1 = 400$ nm) of the two isomers are markedly different. This enables us to generate an absorbance modulation in this layer upon exposure to the two wavelengths. The photochromic properties of this polymer were analyzed by spin coating on a glass slide, irradiating with a Hg lamp, and conducting uv-vis spectroscopy. Figure 2(a) shows the change in absorbance of 200 nm of the polymer measured at 405 nm upon exposure to 405 nm at an intensity of $1.2\ \text{mW/cm}^2$. Figure 2(b) shows the same when the sample was exposed to $20\ \text{mW/cm}^2$ at 546 nm. The choice of wavelengths was constrained by the available lines of the Hg lamp. Nevertheless, they are close enough to wavelengths in our experimental system that the photochromic parameters extracted here may be successfully employed to explain the experimental results as described later. Applying the photokinetic model described in Ref. [14] to the measured data, we extracted the material parameters for the azobenzene polymer. These parameters are listed in Fig. 2. The subscripts A and B refer to the trans and cis isomers, respectively, while the subscripts 1 and 2 refer to λ_1 and λ_2 respectively. The symbols ϵ, ϕ, and k refer to the corresponding molar absorption coefficient, the quantum efficiency and the thermal rate constant, respectively.

Results and discussion.—Scanning-electron micrographs of typical exposed patterns are shown in Figs. 3(a) and 3(b). The period of the lines is identical to the period of the standing wave at λ_2, and it may be

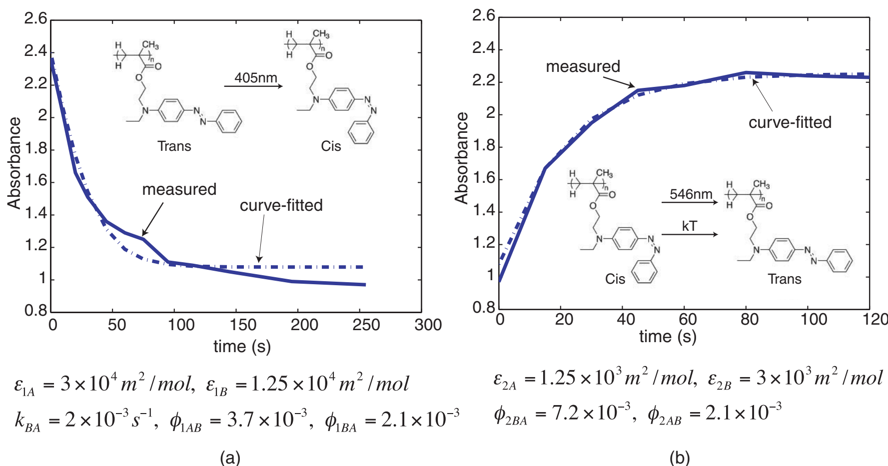

FIG. 2 (color online). Absorbance (at 405 nm) measured as a function of time, when a 200 nm photochromic layer was illuminated by (a) $1.2\ \text{mW/cm}^2$ at 405 nm, and subsequently by (b) $20\ \text{mW/cm}^2$ at 546 nm. The experimental data (solid) are overlaid with the simulation (dashed), which enables the extraction of the photochromic parameters.

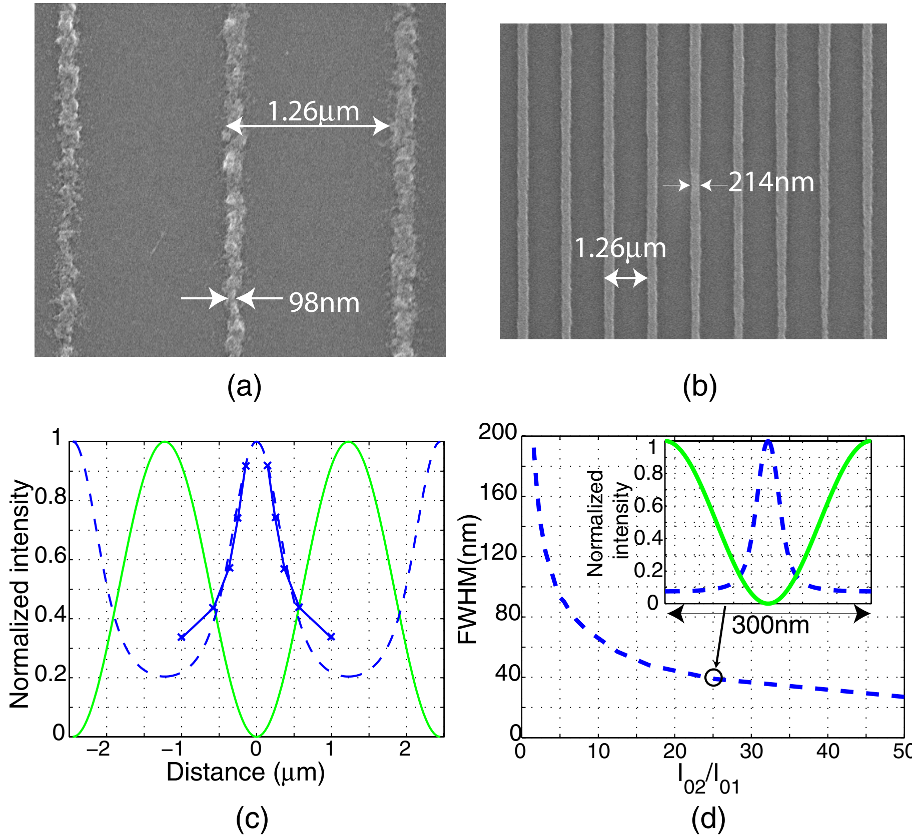

FIG. 3 (color online). (a),(b) Scanning-electron micrographs of lines exposed in negative photoresist. The average linewidth of the middle line in Fig. 3(a) is about 117 nm. The period of the lines is determined by λ_2 and the angle in the Lloyd's mirror setup. (c) Light intensity distribution of the localized fields underneath the AML for a standing-wave period of 2.45 μm. The simulated data is shown with dashed lines. The experimental data is overlaid (solid line) for comparison. (d) FWHM as a function of I_{02}/I_{01} for a standing-wave period of 300 nm. The parameters of the AML listed in Fig. 2 were used in all the simulations.

adjusted by the angle between the incident beam and the Lloyd's mirror. Since PS-4 has almost no sensitivity to $\lambda_2 = 532$ nm, the exposure is exclusively due to the localized light fields at $\lambda_1 = 400$ nm generated by the absorbance modulation in the photochromic overlayer. This situation is analogous to contact photolithography albeit without a rigid photomask. The lines in Fig. 3(b) were formed near the center of the 400 nm beam with an exposure time of about 90 min, whereas those in Fig. 3(a) were formed at the far edges of the blue beam (where the intensity is significantly lower) with an exposure time of about 240 min. The smallest linewidth that we were able to resolve was about 100 nm. This was primarily limited by the thickness of the PS-4 photoresist (150 nm). The significant line-edge roughness evident in Fig. 3(a) is likely due to the underexposure of the chemically-amplified photoresist.

To quantify the spatial structure of the transmitted light at λ_1, we performed exposures at a multitude of exposure times. Assuming a highly nonlinear photoresist exposure and development process, the linewidth measurements as a function of exposure dose accurately map out the intensity distribution of the localized light field [17]. This intensity distribution can be simulated using the model described in Ref. [14]. In fact, this model can be simplified if we assume that the photostationary state is achieved much faster than the overall exposure time, which is true for the situation considered in this Letter. Then, the photostationary absorbance can be calculated by solving the following transcendental equation

$$I_{01}F_1(x)\{\phi_{1AB}\alpha_{1A}(x) - \phi_{1BA}\alpha_{1B}(x)\} = I_{02}(x)F_2(x)\{\phi_{2BA}\alpha_{2B}(x) - \phi_{2AB}\alpha_{2A}(x) + k_{BA}[B]\}, \quad (1)$$

where

$$I_{02}(x) = \left[2I_{02}\sin\left(\frac{\pi}{P}x\right)\right]^2, \quad (2)$$

and

$$\alpha_i = \alpha_{iA} + \alpha_{iB} = [A]\epsilon_{iA}l + [B]\epsilon_{iB}l, \qquad i = 1, 2, \quad (3)$$

where P is the period of the standing wave at λ_2, l is the thickness of the AML, x is the spatial coordinate perpendicular to the lines, $[A]$ and $[B]$ are the concentrations of trans and cis isomers, respectively, and I_{01} and I_{02} are the peak intensities at λ_1 and λ_2, respectively. F is the photokinetic factor given by

$$F_i(x) = \frac{(1 - 10^{-\alpha_i(x)})}{\alpha_i(x)}, \qquad i = 1, 2. \quad (4)$$

Finally, the intensity of the localized light field at λ_1 is given by

$$I_1(x) = I_{01}10^{-\alpha_1(x)}. \quad (5)$$

Using the photochromic parameters listed in Fig. 2, and the measured ratio of intensities (I_{02}/I_{01}) near the optical axis, the intensity distribution of the localized light field was calculated and plotted with dashed lines in Fig. 3(c). The period of the standing wave at λ_2, in this case, was 2.46 μm. The experimental data are also plotted for comparison. The sinusoidal solid curve shows the standing wave at λ_2 that was incident on the AML. The excellent agreement between experiment and theory confirms that the spatial confinement of light is achieved via absorbance modulation.

In absorbance modulation, light localization is achieved by the generation of low-absorbance regions at the nodes of the standing wave at λ_2. As was pointed out earlier [12,14,18], the width of this low-absorbance region can be decreased by increasing I_{02}/I_{01}. To illustrate this point, we calculated the full-width at half-maximum (FWHM) of the exposed line at λ_1 as a function of I_{02}/I_{01} for a standing-wave period of 300 nm, and plotted in Fig. 3(d). The FWHM shows a characteristic nonlinear behavior and can reach values far below the diffraction limit imposed by either λ_1 or λ_2.

Conclusion.—In this Letter, we demonstrated the localization of light fields using a thin photochromic overlayer, whose absorbance was modulated by a standing wave at $\lambda_2 = 532$ nm and a uniform beam at $\lambda_1 = 400$ nm. The localization is due to the generation of low-absorbance regions in the photochromic layer, whose width can be significantly below the diffraction limit. This will enable the generation of optical near fields by projecting images from the far field, thereby impacting applications ranging from scanning-probe microscopies to nanopatterning and particle manipulation.

The authors would like to thank Henry Smith for critical comments on this Letter, Michael Walsh for assistance with the Lloyd's mirror setup, and Tom O'Reilly for helpful suggestions regarding PS-4 photoresist.

*Electronic address: rmenon@nano.mit.edu

[1] H. I. Smith, R. Menon, A. Patel, D. Chao, M. Walsh, and G. Barbastathis, Microelectron. Eng. **83**, 956 (2006).
[2] S. Sun and G. J. Leggett, Nano Lett. **4**, 1381 (2004).
[3] A. Lewis, H. Taha, A. Strinkovski, A. Manevitch, A. Khatchatouriants, R. Dehkter, and E. Ammann, Nat. Biotechnol. **21**, 1378 (2003).
[4] J. G. Goodberlet and H. Kavak, Appl. Phys. Lett. **84**, 4780 (2004).
[5] B. W. Smith, Y. Fan, J. Zhou, N. Laerty, and A. Estro, Proc. SPIE-Int. Soc. Opt. Eng. **6154**, 61540A (2006).
[6] T. M. Bloomstein, M. F. Marchant, S. Deneault, D. E. Hardy, and M. Rothschild, Opt. Express **14**, 6434 (2006).
[7] J. B. Pendry, Phys. Rev. Lett. **85**, 3966 (2000).
[8] R. J. Blaikie, D. O. S. Melville, and M. M. Alkaisi, Microelectron. Eng. **83**, 723 (2006).
[9] N. Fang, H. Lee, C. Sun, and X. Zhang, Science **308**, 534 (2005).
[10] T. Ito, M. Ogino, T. Yamada, Y. Inao, T. Yamaguchi, N. Mizutani, and R. Kuroda, J. Photopolym. Sci. Technol. **18**, 435 (2005).
[11] T. Ito, T. Yamada, Y. Inao, T. Yamaguchi, N. Mizutani, and R. Kuroda, Appl. Phys. Lett. **89**, 033113 (2006).
[12] S. W. Hell, Phys. Lett. A **326**, 140 (2004).
[13] G. Donnert, J. Keller, R. Medda, M. A. Andrei, S. O. Rizolli, R. Luhrmann, R. Jahn, C. Eggeling, and S. W. Hell, Proc. Natl. Acad. Sci. U.S.A. **103**, 11 440 (2006).
[14] R. Menon and H. I. Smith, J. Opt. Soc. Am. A **23**, 2290 (2006).
[15] M.-S. Ho, A. Natansohn, C. Barrett, and P. Rochon, Can. J. Chem. **73**, 1773 (1995).
[16] C. Barrett, A. Natansohn, and P. Rochon, Chem. Mater. **7**, 899 (1995).
[17] R. Menon, D. Gil, and H. I. Smith, J. Opt. Soc. Am. A **23**, 567 (2006).
[18] M. Hofmann, C. Eggeling, S. Jakobs, and S. W. Hell, Proc. Natl. Acad. Sci. U.S.A. **102**, 17 565 (2005).